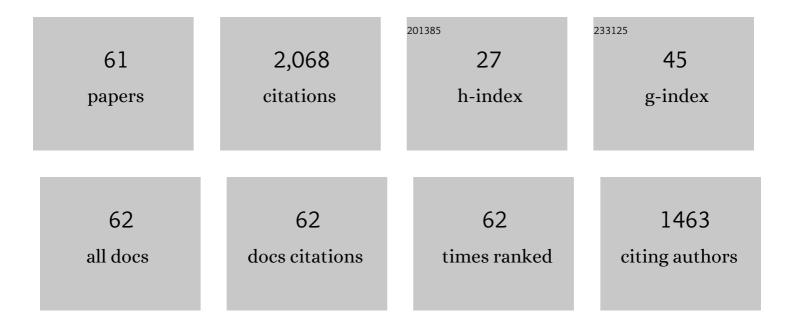
List of Publications by Year in descending order

Source: https://exaly.com/author-pdf/1793152/publications.pdf Version: 2024-02-01



Detd Zeman

#	Article	IF	CITATIONS
1	Effect of total and oxygen partial pressures on structure of photocatalytic TiO2 films sputtered on unheated substrate. Surface and Coatings Technology, 2002, 153, 93-99.	2.2	201
2	ZrN/Cu nanocomposite film—a novel superhard material. Surface and Coatings Technology, 1999, 120-121, 179-183.	2.2	200
3	Structure and properties of hard and superhard Zr–Cu–N nanocomposite coatings. Materials Science & Engineering A: Structural Materials: Properties, Microstructure and Processing, 2000, 289, 189-197.	2.6	139
4	Thermal stability of alumina thin films containing γ-Al2O3 phase prepared by reactive magnetron sputtering. Applied Surface Science, 2010, 257, 1058-1062.	3.1	115
5	Reactive magnetron sputtering of hard Si–B–C–N films with a high-temperature oxidation resistance. Journal of Vacuum Science and Technology A: Vacuum, Surfaces and Films, 2005, 23, 1513-1522.	0.9	76
6	Amorphous Zr-Cu thin-film alloys with metallic glass behavior. Journal of Alloys and Compounds, 2017, 696, 1298-1306.	2.8	73
7	Hard amorphous nanocomposite coatings with oxidation resistance above 1000°C. Advances in Applied Ceramics, 2008, 107, 148-154.	0.6	68
8	Self-cleaning and antifogging effects of TiO2 films prepared by radio frequency magnetron sputtering. Journal of Vacuum Science and Technology A: Vacuum, Surfaces and Films, 2002, 20, 388-393.	0.9	67
9	Nano-scaled photocatalytic TiO2 thin films prepared by magnetron sputtering. Thin Solid Films, 2003, 433, 57-62.	0.8	66
10	Structure and properties of magnetron sputtered Zr–Si–N films with a high (≥25 at.%) Si content. Thin Solid Films, 2005, 478, 238-247.	0.8	57
11	Properties of magnetron sputtered Al–Si–N thin films with a low and high Si content. Surface and Coatings Technology, 2008, 202, 3485-3493.	2.2	56
12	Properties of reactively sputtered W–Si–N films. Surface and Coatings Technology, 2006, 200, 3886-3895.	2.2	50
13	Hard a-Si <sub>3</sub> N <sub>4</sub> /MeN <sub>x</sub> Nanocomposite Coatings with High Thermal Stability and High Oxidation Resistance. Solid State Phenomena, 2007, 127, 31-36.	0.3	44
14	Difference in high-temperature oxidation resistance of amorphous Zr–Si–N and W–Si–N films with a high Si content. Applied Surface Science, 2006, 252, 8319-8325.	3.1	43
15	High-temperature oxidation resistance of Ta–Si–N films with a high Si content. Surface and Coatings Technology, 2006, 200, 4091-4096.	2.2	42
16	Effect of the gas mixture composition on high-temperature behavior of magnetron sputtered Si–B–C–N coatings. Surface and Coatings Technology, 2008, 203, 466-469.	2.2	42
17	Structure and microhardness of magnetron sputtered ZrCu and ZrCu-N films. Vacuum, 1999, 52, 269-275.	1.6	41
18	Thermal stability of magnetron sputtered Si–B–C–N materials at temperatures up to 1700°C. Thin Solid Films, 2010, 519, 306-311.	0.8	41

#	Article	IF	CITATIONS
19	Thermal stability of magnetron sputtered Zr–Si–N films. Surface and Coatings Technology, 2006, 201, 3368-3376.	2.2	40
20	Physical properties and high-temperature oxidation resistance of sputtered Si[sub 3]N[sub 4]â^•MoN[sub x] nanocomposite coatings. Journal of Vacuum Science & Technology an Official Journal of the American Vacuum Society B, Microelectronics Processing and Phenomena, 2005, 23, 1568.	1.6	36
21	Microstructure characterization of high-temperature, oxidation-resistant Si-B-C-N films. Thin Solid Films, 2013, 542, 167-173.	0.8	35
22	Hard and superhard nanocomposite Al–Cu–N films prepared by magnetron sputtering. Surface and Coatings Technology, 2001, 142-144, 603-609.	2.2	33
23	Physical and mechanical properties of sputtered Ta–Si–N films with a high (≥40 at %) content of Si. Journal of Vacuum Science and Technology A: Vacuum, Surfaces and Films, 2004, 22, 646.	0.9	33
24	Hydrogen gas sensing properties of WO3 sputter-deposited thin films enhanced by on-top depositedACuO nanoclusters. International Journal of Hydrogen Energy, 2018, 43, 22756-22764.	3.8	31
25	Effect of Si addition on mechanical properties and high temperature oxidation resistance of Ti–B–Si hard coatings. Surface and Coatings Technology, 2014, 240, 48-54.	2.2	29
26	Superior high-temperature oxidation resistance of magnetron sputtered Hf–B–Si–C–N film. Ceramics International, 2016, 42, 4853-4859.	2.3	28
27	Magnetron sputtered Si–B–C–N films with high oxidation resistance and thermal stability in air at temperatures above 1500 °C. Journal of Vacuum Science and Technology A: Vacuum, Surfaces and Films, 2008, 26, 1101-1108.	0.9	27
28	Effect of positive pulse voltage in bipolar reactive HiPIMS on crystal structure, microstructure and mechanical properties of CrN films. Surface and Coatings Technology, 2020, 393, 125773.	2.2	27
29	Hard nanocrystalline Zr–B–C–N films with high electrical conductivity prepared by pulsed magnetron sputtering. Surface and Coatings Technology, 2013, 215, 186-191.	2.2	23
30	Morphology and Microstructure of Hard and Superhard Zr–Cu–N Nanocomposite Coatings. Japanese Journal of Applied Physics, 2002, 41, 6529-6533.	0.8	22
31	Pulsed reactive magnetron sputtering of high-temperature Si–B–C–N films with high optical transparency. Surface and Coatings Technology, 2013, 226, 34-39.	2.2	22
32	Hard multifunctional Hf–B–Si–C films prepared by pulsed magnetron sputtering. Surface and Coatings Technology, 2014, 257, 301-307.	2.2	20
33	Ti-Si-N Films with a High Content of Si. Plasma Processes and Polymers, 2007, 4, S574-S578.	1.6	19
34	Hard Nanocomposite Coatings. , 2014, , 325-353.		19
35	Non-isothermal kinetics of phase transformations in magnetron sputtered alumina films with metastable structure. Thermochimica Acta, 2013, 572, 85-93.	1.2	18
36	Formation of crystalline Al–Ti–O thin films and their properties. Surface and Coatings Technology, 2008, 202, 6064-6069.	2.2	17

#	Article	IF	CITATIONS
37	Effect of Al Addition on Structure and Properties of Sputtered TiC Films. Plasma Processes and Polymers, 2007, 4, S6-S10.	1.6	14
38	Thermally activated transformations in metastable alumina coatings prepared by magnetron sputtering. Surface and Coatings Technology, 2014, 240, 7-13.	2.2	14
39	Protective Zr-containing SiO2 coatings resistant to thermal cycling in air up to 1400°C. Surface and Coatings Technology, 2009, 203, 1502-1507.	2.2	13
40	Molecular dynamics and experimental study of the growth, structure and properties of Zr–Cu films. Journal of Alloys and Compounds, 2020, 828, 154433.	2.8	12
41	Microstructure evolution in amorphous Hf-B-Si-C-N high temperature resistant coatings after annealing to 1500 °C in air. Scientific Reports, 2019, 9, 3603.	1.6	11
42	Impact of Al or Si addition on properties and oxidation resistance of magnetron sputtered Zr–Hf–Al/Si–Cu metallic glasses. Journal of Alloys and Compounds, 2019, 772, 409-417.	2.8	10
43	Effect of annealing on structure and properties of Ta–O–N films prepared by high power impulse magnetron sputtering. Ceramics International, 2019, 45, 9454-9461.	2.3	10
44	Tuning properties and behavior of magnetron sputtered Zr-Hf-Cu metallic glasses. Journal of Alloys and Compounds, 2018, 739, 848-855.	2.8	8
45	Study of the high-temperature oxidation resistance mechanism of magnetron sputtered Hf7B23Si17C4N45 film. Journal of Vacuum Science and Technology A: Vacuum, Surfaces and Films, 2018, 36, .	0.9	7
46	On crystallization and oxidation behavior of Zr54Cu46 and Zr27Hf27Cu46 thin-film metallic glasses compared to a crystalline Zr54Cu46 thin-film alloy. Journal of Non-Crystalline Solids, 2018, 500, 475-481.	1.5	7
47	Self-formation of dual glassy-crystalline structure in magnetron sputtered W–Zr films. Vacuum, 2021, 187, 110099.	1.6	7
48	Three-Layer PdO/CuWO4/CuO System for Hydrogen Gas Sensing with Reduced Humidity Interference. Nanomaterials, 2021, 11, 3456.	1.9	7
49	Metastable structures in magnetron sputtered W–Zr thin-film alloys. Journal of Alloys and Compounds, 2021, 888, 161558.	2.8	6
50	Thermal stability of structure, microstructure and enhanced properties of Zr–Ta–O films with a low and high Ta content. Surface and Coatings Technology, 2018, 335, 95-103.	2.2	5
51	Extraordinary high-temperature behavior of electrically conductive Hf7B23Si22C6N40 ceramic film. Surface and Coatings Technology, 2020, 391, 125686.	2.2	5
52	Reactive HiPIMS deposition of Al-oxide thin films using W-alloyed Al targets. Surface and Coatings Technology, 2021, 422, 127467.	2.2	5
53	Time-averaged and time-resolved ion fluxes related to reactive HiPIMS deposition of Ti-Al-N films. Surface and Coatings Technology, 2021, 424, 127638.	2.2	5
54	Oxidation of Sputtered Cu, Zr, ZrCu, ZrO2, and Zr-Cu-O Films during Thermal Annealing in Flowing Air. Plasma Processes and Polymers, 2007, 4, S536-S540.	1.6	4

#	Article	IF	CITATIONS
55	Nanoindentation and microbending analyses of glassy and crystalline Zr( Hf) Cu thin-film alloys. Surface and Coatings Technology, 2020, 399, 126139.	2.2	4
56	Thermal stability and transformation phenomena in magnetron sputtered Al–Cu–O films. Ceramics International, 2015, 41, 6020-6029.	2.3	3
57	Tuning Stoichiometry and Structure of Pd-WO3â^'x Thin Films for Hydrogen Gas Sensing by High-Power Impulse Magnetron Sputtering. Materials, 2020, 13, 5101.	1.3	3
58	Enhancement of high-temperature oxidation resistance and thermal stability of hard and optically transparent Hf–B–Si–C–N films by Y or Ho addition. Journal of Non-Crystalline Solids, 2021, 553, 120470.	1.5	3
59	Microstructure of High Temperature Oxidation Resistant Hf6B10Si31C2N50 and Hf7B10Si32C2N44 Films. Coatings, 2020, 10, 1170.	1.2	2
60	Hard a-Si <sub>3</sub> N <sub>4</sub> /MeN <sub>x</sub> Nanocomposite Coatings with High Thermal Stability and High Oxidation Resistance. Solid State Phenomena, 0, , 31-36.	0.3	2
61	Bixbyite-Ta2N2O film prepared by HiPIMS and postdeposition annealing: Structure and properties. Journal of Vacuum Science and Technology A: Vacuum, Surfaces and Films, 2020, 38, .	0.9	1